Monodisperse Poly(lactide-*co*-glycolic acid)-Based Nanocarriers for Gene Transfection

Jeong Hoon Byeon, Hee-Kwon Kim, Jeffrey T. Roberts*

This contribution describes a simple, aerosol-based method for fabricating monodisperse particles containing mixtures of poly(lactide-*co*-glycolic acid) [PLGA], protamine sulfate (Prot), and poly(L-lysine) [PLL] as nanocarriers for gene transfection. Aqueous solutions of PLGA, Prot, and PLL were collison-atomized, and the resulting aerosolized droplets were dried "on the fly" to form solid particles, which then were electrostatically size-classified into 50, 100, and 200 nm mobility diameter samples. Measurements of cell viability and transfection reveal that the fabricated nanocarriers have a lower cytotoxicity (>85% in cell viability) and a higher transfection efficiency [$>8.7 \times 10^5$ in relative light units (RLU) mg^{-1}] than does 25 kDa polyethyleneimine (≈50% and 6.8×10^5 RLU mg^{-1}).

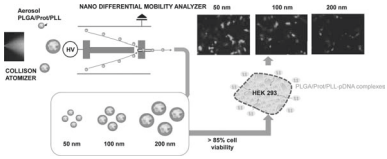

1. Introduction

Polymeric nanoparticles (1–200 nm diameter range) can be used therapeutically as nanocarriers drugs or biologically active material.[1] Nanocarriers prepared using biocompatible and biodegradable poly(lactide-*co*-glycolic acid) [PLGA] polymers have attracted much attention as suitable candidates for therapeutic applications because of favorable physicochemical characteristics, including safety, stability, relative ease of large-scale production, and lack of intrinsic immunogenicity.[2] Many formulations based on polymer-based systems exist as colloidal liquids, usually synthesized using time-consuming batch, wet chemical processes and are generally stable only for short periods of time. Moreover, some polymer systems are designed to be gradually degradable by hydrolysis, making long-term storage in liquid form not a viable option.[3] In addition, many formulations are unstable as liquid suspensions for a variety of reasons, including degradation of the carrier and/or active substance, formation of insoluble aggregates, and unwanted loss of bioactivity.[4] One approach for overcoming such stability limitations is to formulate and store dry powders.

In contrast to classical wet chemical methods, aerosol processing involves a much more limited number of preparation steps. It also produces material continuously, allowing for a straightforward collection of powders and generating low waste.[5] The field of therapeutic aerosol bioengineering, driven originally by the goal of developing inhalable insulin, is now expanding to address medical needs ranging from respiratory to systemic diseases.[6] Dry particles can be formulated in the aerosol state by atomizing liquid solutions in an appropriate carrier gas and removing solvent from the resulting particles.[5b] Processing is highly reproducible, relatively easy to scale up, and offers uniform particle size distributions.[5c] The method is mostly used in the pharmaceutical industry to generate spherical microparticles for treating pulmonary diseases,[7] although it also can be used to generate a variety of nano-sized polymeric particles,[1b] some of which have been proven to be effective therapeutic carriers.[7b]

The size and surface characteristics of a polymer particle inevitably influence therapeutic capabilities. The

Dr. J. H. Byeon,[a] Prof. J. T. Roberts
Department of Chemistry, Purdue University, IN 47907, USA
E-mail: jtrob@purdue.edu
Dr. H.-K. Kim[a]
Department of Molecular and Medical Pharmacology, University of California Los Angeles, CA 90095, USA
[a] These authors contributed equally to this work.

DOI: 10.1002/marc.201200369

ability to control the size and morphology distribution of particles in a polymer formulation thus translates into the ability to control release properties.[8] Size and surface modification have been effective strategies for enhancing particle utility, increasing circulation time for transport across physical barriers, and prolonging residence time at an active site.[8] For example, release efficiency generally increases with surface-to-volume ratio, making monodispersity a critical element of dosage control. Release is also enhanced by surface diffusion or erosion. Size and surface control can sometimes be achieved in a wet chemical process by controlling synthesis conditions, but non-uniform distributions and chemical heterogeneity are more often the case. Low cytotoxicity and high gene transfection efficiency are also critical issues in designing current delivery carriers.[2a]

The purpose of the present work is to report the fabrication of monodisperse nanoparticles containing mixtures of the copolymer PLGA, the homopolymer poly(L-lysine) [PLL], and the drug protamine sulfate (Prot) using a one-step aerosol method. PLGA, which has favorable biodegradable and biocompatible properties, is widely used therapeutically. The cationic components of the particles, Prot, and PLL, have been widely applied in delivery carriers because they electrostatically interact with negatively charged DNA and help to enhance the affinity for proteins and cells.[9] In this work, the applicability and suitability of these particles as nanocarriers are explored. In particular, critical physicochemical properties (size, morphology, and surface charge) and biological properties [in vitro cytotoxicity and transfection efficiency in human embryonic kidney (HEK) 293 cells] of the gene loaded nanocarriers are evaluated.

2. Results and Discussion

Figure 1 summarizes the size distributions of particles formed by collision atomizing an aqueous solution of PLGA, and an aqueous solution of PLGA, Prot, and PLL. The geometric mean diameter (GMD), geometric standard deviation (GSD), and total number concentration (TNC) of the pure PLGA particles are 100.1 nm, 1.75, and 2.06×10^7 particles cm^{-3}, respectively, as shown in Table 1S (Supporting Information). Analogous data for particles derived from the aqueous mixtures are 125.2 nm, 1.77, and 2.06×10^7 particles cm^{-3}, respectively. The distribution of the PLGA/Prot/PLL particles is slightly shifted to larger sizes, consistent with incorporation of the two new components Prot and PLL. The size-classified carriers show substantially narrower GSD values (≈1.25) than the non-classified cases (1.77). Mobility classification does result in some material loss.[10] The number concentration of particles classified at 50 nm is 4.9% of the concentration of non-classified particles. For particles classified at 100 and 200 nm, the values are 10.2% and 3.4%, respectively.

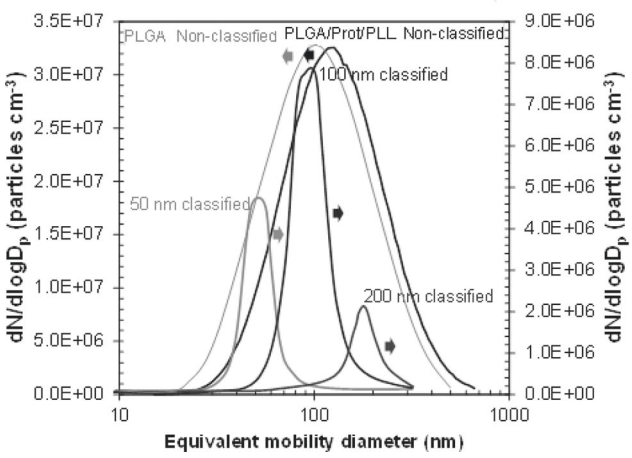

Figure 1. Size distributions of non-classified PLGA and PLGA/Prot/PLL, and size-classified PLGA/Prot/PLL nanocarriers. The size-classified carriers are differentgray(50, 100, and 200 nm) lines.

Figure 2 shows typical TEM images of PLGA/Prot/PLL particles, collected both before and after mobility classification. The PLGA/Prot/PLL particles exhibit similar uniform spherical shapes, with smooth surfaces. Particles are also well separated. The formation of dense solid particles (second image in Figure 2) is facilitated by slow convective drying, where the time for the liquid to evaporate is greater than the time required for supersaturated particles at the liquid–vapor interface to migrate back toward a droplet center. The mean mode diameter of the non-classified PLGA/Prot/PLL nanocarrier particles is 134 ± 8.2 nm. The same data for the 50, 100, and 200 nm classified cases are 53 ± 2.2, 104 ± 3.2, and 199 ± 8.6 nm, respectively, and

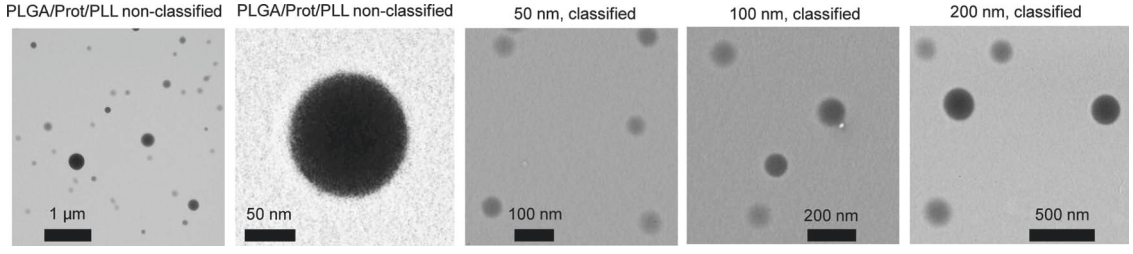

Figure 2. TEM images of non- and size-classified PLGA/Prot/PLL carriers.

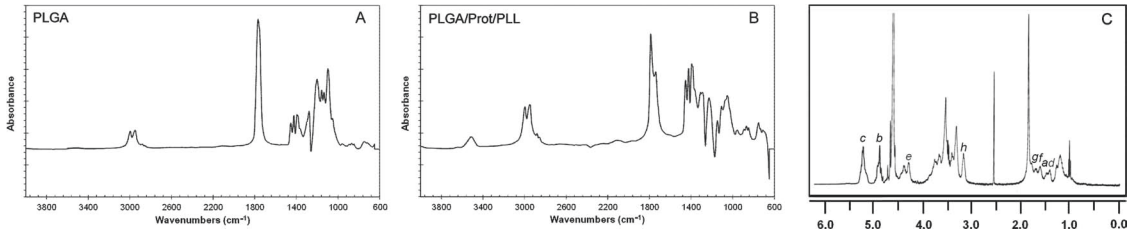

Figure 3. IR spectra of (A) pure PLGA and (B) PLGA/Prot/PLL carrier samples. NMR spectrum (C) of a PLGA/Prot/PLL carrier sample.

these data are in good agreement with the data shown in Figure 1. Particles are also spherical in shape, and nearly monodisperse.

The number density of the PLGA/Prot/PLL carriers varies with size and the value for the 50 nm classified case is the highest well described by the following equation:

$$n = \frac{6m_{\text{PLGA/ Prot/ PLL}}}{\pi D_p^3 \rho_{\text{PLGA/ Prot/ PLL}}} \quad (1)$$

where n is the number of PLGA/Prot/PLL carriers, $m_{\text{PLGA/Prot/PLL}}$ is the unit mass (1 mg) of PLGA/Prot/PLL, D_p is the average diameter of PLGA/Prot/PLL, and $\rho_{\text{PLGA/Prot/PLL}}$ is the density of PLGA/Prot/PLL (1.26 g cm^{-3}). The estimated numbers of PLGA/Prot/PLL carriers are approximately 0.08, 1.23, 0.15, and 0.02 $\times$ 10^{13} mg^{-1} for the cases of the non-classified, and 50, 100, and 200 nm classified particles, respectively, and the corresponding specific surface area of the cases are approximately 38.6, 96.8, 48.4, and 24.2 m^2 g^{-1}, respectively.

FTIR spectra of collected PLGA particles (Figure 3A) show absorbance peaks at 1087 and 1187 cm^{-1} (C–O stretch), 1389 cm^{-1} (CH bend), 1759 cm^{-1} (ester C=O), 2946 cm^{-1} (CH_2 bend), and 2960 cm^{-1} (CH_3 bend).[11] For a sample of collected PLGA/Prot/PLL particles (Figure 3B), the absorption peaks at 1033 and 1190 cm^{-1} are attributed to the symmetrical and asymmetrical stretching vibrations of S=O, respectively, arising from incorporated Prot. Other features include characteristic absorption peaks at around 3400 cm^{-1} (related to–NH_2 and O–H groups), and the 1730 cm^{-1} peaks assigned to carbonyl and ester groups (NHCOO stretching combined with ester COO stretching), originating from Prot and PLL.[11c] The PLGA/Prot/PLL sample still showed the peak positions at 1,759 cm^{-1} (C=O ester), 2946 cm^{-1} (CH_2 bend), and 2960 cm^{-1} (CH_3 bend), which were also observed for the pure PLGA sample, implying that the PLGA/Prot/PLL was a mixture form of PLGA, Prot, and PLL. Figure 3C shows on ^1H NMR spectrum, obtained of a particle sample that was suspended in D_2O and then subjected to ultrasound treatment for 10 s. Characteristic peaks of PLGA are obtained at 1.45 ppm δ (*a*), 4.87 ppm δ (*b*), and 5.21 ppm δ (*c*).[12] Peaks at 1.35 and 4.20 ppm are attributed to protons in the lysine segment.[13] The peaks labeled *f*, *g*, and *h* at 1.59, 1.74, and 3.13 ppm, δ are assigned to protamine sulfate.[14] Minor differences between the IR and NMR spectra of pure PLGA and the PLGA/Prot/PLL are taken as evidence for mixing of PLGA, Prot, and PLL. It can be inferred that the pDNA could be completely complexed with the carriers by ionic binding (because a positive surface charge allows an electrostatic interaction between negatively charged cellular membranes and the positively charged complexes). The zeta potential of PLGA/pDNA is initially negatively charged (due to the existence of carboxyl groups on PLGA), at approximately −20.7 mV, but became positively charged, as shown in Table 2S (Supporting Information). The values of the PLGA/Prot/PLL–pDNA complexes confirm the net positive charge, which is attributed primarily to protonated amino groups.[2e]

Agarose gel retardation assay was carried out to confirm whether pDNA would associate with the cationic PLGA/Prot/PLL nanocarriers, and to qualitatively investigate the optimal weight ratio (0.1, 0.5, 1.0, 5.0, and 10.0) of PLGA/Prot/PLL to pDNA for binding efficiency. As shown in Figure 1S (Supporting Information), it is observed that naked DNA (lane 1) migrated to the positive electrode under the electric field. At a ratio of 0.5 or above, almost all DNA combined with PLGA/Prot/PLL with little free DNA visibly escaping in lanes 3–6.

The cytotoxicity of the complexes at the chosen sizes was evaluated using an MTS assay in HEK 293 cells. Results were compared to PEI (Figure 4A), which has been widely applied in biomedical applications because of its excellent properties such as biocompatibility, nontoxicity, and biodegradability.[15] Results show that cell viability is >85% for all the tested PLGA/Prot/PLL carriers, while a lower viability (~50%) was observed for PEI. This implies that PLGA/Prot/PLL may be non-cytotoxic in a clinical context. In addition, there are no significant differences of cytotoxicity between the PLGA/Prot/PLL samples. The cytotoxicity of cationic polymers is considered to be a consequence of damage from interactions with plasma membranes or other cellular compartments.[16] Therefore, the fact that the cell viability of all PLGA/Prot/PLL carriers is >85% suggests that the charge density of PLGA/Prot/PLL is acceptable in.vitro. Differences in transfection ability among these PLGA/Prot/PLL carriers were further confirmed by a luciferase assay. The ability of the PLGA/Prot/PLL carriers to transfect HEK 293 cells using

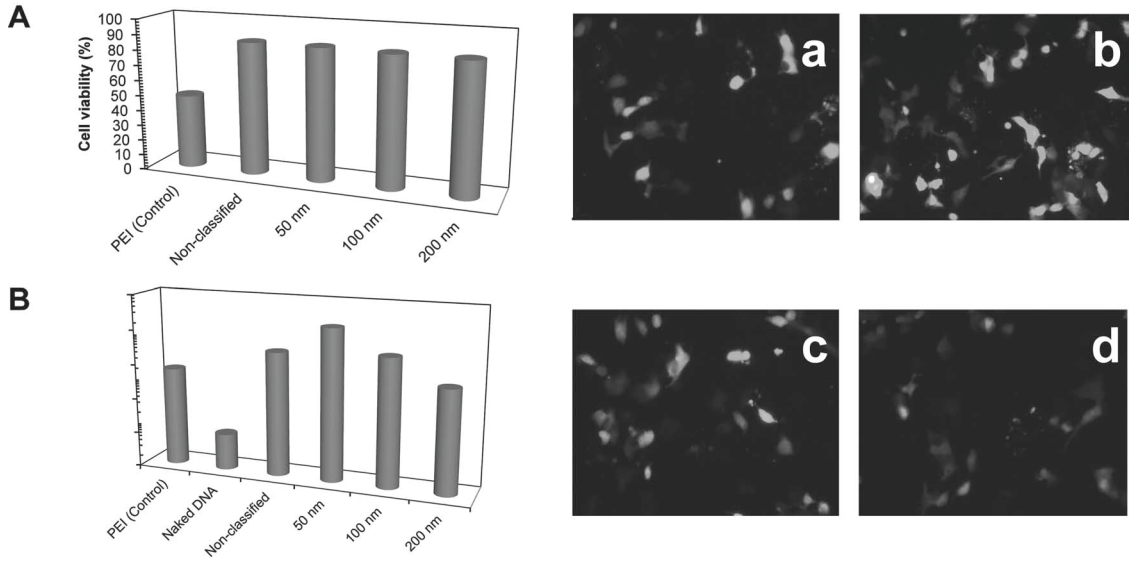

Figure 4. Results of (A) cytotoxicity of PLGA/Prot/PLL carriers in HEK 293 cells, (B) transfection efficiency, and (C) transfection fluorescence imaging of PLGA/Prot/PLL carriers in HEK 293 cells for 24 h. (C–a) to (C–d) are the non-classified, and the 50, 100, and 200 nm classified PLGA/Prot/PLL carriers, respectively.

pDNA containing the luciferase and the green fluorescent protein (GFP) gene was investigated and compared to PEI/pDNA complexes. From the results of the amount of luciferase protein (Figure 4B), it is shown that naked DNA was barely transfected in HEK 293 cells, whereas both PLGA/Prot/PLL and PEI complexes could achieve intracellular transfection. Compared with PEI complexes, the transfection of PLGA/Prot/PLL complexes still exhibits a higher expression of up to 2.1×10^7 RLU mg^{-1} (for the 50 nm classified case). The efficiency increased with decreasing carrier size, implying that the transfection efficiency may be controlled by classifying the carrier size. In previous reports, PLGA nanocarriers with smaller sizes below 100 nm have been shown to have higher transfection efficiencies than those of larger sizes.[2,17] In the present cases, the carrier size demonstrated a key role in determining the level of transfection efficiency because the zeta potential did not show a remarkable difference between the samples [the 200 nm classified (26.7 mV) case is slightly higher than 50 nm classified (23.2 mV) case]. Figure 4C shows fluorescence images of HEK 293 cells for the PLGA/Prot/PLL complexes derived from GFP expression, which further confirmed the transfection and differences between the PLGA/Prot/PLL complexes (i.e., sizes). The higher efficiency of the PLGA/Prot/PLL carriers may be ascribed to the combination of high affinity between the luciferase and PLGA/Prot/PLL complexes and the relatively small size (i.e., especially 50 nm, which corresponds to relatively high surface area, 96.8 m^2 g^{-1}) of the PLGA/Prot/PLL carriers [cf. ≈120 nm for PEI (Figure 2S, Supporting Information) and ≈125 nm for non-classified PLGA/Prot/PLL carriers].

3. Conclusion

For the first time, one-step aerosol fabrication of monodisperse PLGA-based mixture polymer nanocarriers has been used in in vitro cytotoxicity and transfection. Aqueous solutions of PLGA, Prot, and PLL were collison-atomized, and the resulting aerosolized droplets were dried to form solid particles, which then were electrostatically size-classified into 50, 100, and 200 nm mobility diameter samples. Agarose gel retardation assay confirms that collected particles bind pDNA. It exhibited a lower cytotoxicity and a higher transfection efficiency in HEK 293 cells compared to the PEI/pDNA complexes. These results further establish aerosol processing as an efficient, green, scalable fabrication, which is generalizable to an extraordinarily broad range of promising nanocarriers.

Supporting Information

Supporting Information is available from the Wiley Online Library or from the author.

Acknowledgements: This work was partially supported by NSF grant CHE-0924431.

Received: May 25, 2012; Revised: June 26, 2012; Published online: July 25, 2012; DOI: 10.1002/marc.201200369

Keywords: gene transfection; monodisperse; nanoparticles; particle size distribution; poly(lactide-*co*-glycolic acid)-based nanocarriers

[1] a) J. Kreuter, *J. Control. Release* **1991**, *16*, 169; b) C. B. Packhaeuser, K. Lahnstein, J. Sitterberg, T. Schmehl, T. Gessler, U. Bakowsky, W. Seeger, T. Kissel, *Pharm. Res.* **2009**, *26*, 129; c) J. M. M. Gómez, N. Csaba, S. Fischer, A. Sichelstiel, T. M. Kündig, B. Gander, P. Johansen, *J. Control. Release* **2008**, *130*, 161.
[2] a) C. Fu, X. Sun, D. Liu, Z. Chen, Z. Lu, N. Zhang, *Int. J. Mol. Sci.* **2011**, *12*, 1371; b) D. Mishra, H. C. Kang, Y. H. Bae, *Biomaterials* **2011**, *32*, 3845; c) G. F. Liang, Y. L. Zhu, B. Sun, F. H. Hu, T. Tian, S. C. Li, Z. D. Xiao, *Nanoscale Res. Lett.* **2011**, *6*, 447; d) R. de Lima, A. d. E. S. Pereira, R. M. Porto, L. F. Fraceto, *J. Polym. Environ.* **2011**, *19*, 196; e) K. Tahara, S. Furukawa, H. Yamamoto, Y. Kawashima, *Int. J. Pharm.* **2010**, *392*, 311; f) J. S. Blum, W. M. Saltzman, *J. Control. Release* **2008**, *129*, 66; g) B. Almería, W. Deng, T. M. Fahmy, A. Gomez, *J. Colloid Interface Sci.* **2010**, *343*, 125.
[3] a) D. Q. M. Craig, *Int. J. Pharm.* **2002**, *231*, 131; b) V. Bulmus, Y. Chan, Q. Nguyen, H. L. Tran, *Macromol. Biosci.* **2007**, *7*, 446.
[4] a) M. d. C. Molina, S. D. Allison, T. J. Anchordoquy, *J. Pharm. Sci.* **2001**, *90*, 1445; b) G. M. Flores-Fernández, R. J. Solá, K. Griebenow, *J. Pharm. Pharmacol.* **2009**, *61*, 1555; c) C. J. Thompson, D. Hansford, S. Higgins, C. Rostron, G. A. Hutcheon, D. L. Munday, *J. Microencapsul.* **2009**, *26*, 676; d) C. Miene, S. Klenow, S. Veeriah, E. Richling, M. Glei, *Mol. Nutr. Food Res.* **2009**, *53*, 1254.
[5] a) T. Buranda, J. Huang, G. V. Ramarao, L. K. Ista, R. S. Larson, T. L. Ward, L. A. Sklar, G. P. Lopez, *Langmuir* **2003**, *19*, 1654; b) M.-I. Ré, *Dry. Technol.* **2006**, *24*, 433; c) K. Rizi, R. J. Green, M. Donaldson, A. C. Williams, *J. Pharm. Sci.* **2011**, *100*, 566; d) H.-K. Chan, *Colloid Surf. A–Physicochem. Eng. Asp.* **2006**, *284–285*, 50.
[6] D. A. Edwards, C. Dunbar, *Annu. Rev. Biomed. Eng.* **2002**, *4*, 93.
[7] a) M. B. Dolovich, R. Dhand, *Lancet* **2011**, *377*, 1032; b) K. Hadinoto, P. Phanapavudhikul, Z. Kewu, R. B. H. Tan, *Int. J. Pharm.* **2007**, *333*, 187.
[8] a) Y.-H. Lee, F. Mei, M.-Y. Bai, S. Zhao, D.-R. Chen, *J. Control. Release* **2010**, *145*, 58; b) J. C. Sung, B. L. Pulliam, D. A. Edwards, *Trends Biotechnol.* **2007**, *25*, 563; c) J. Xie, L. K. Lim, Y. Phua, J. Hua, C.-H. Wang, *J. Colloid Interface Sci.* **2006**, *302*, 103.
[9] a) X. Sun, N. Zhang, *Mini. Rev Med. Chem.* **2010**, *10*, 108; b) J. H. Jeong, T. G. Park, *J. Control. Release* **2002**, *82*, 159; c) Y.-C. Chung, W.-Y. Hsieh, T.-H. Young, *Biomaterials* **2010**, *31*, 4194; d) J. Dai, S. Zou, Y. Pei, D. Cheng, H. Ai, X. Shuai, *Biomaterials* **2011**, *32*, 1694.
[10] a) J. H. Byeon, J. T. Roberts, *ACS Appl. Mater. Interfaces* **2012**, *4*, 2515; b) J. H. Byeon, J. H. Ji, J. H. Park, K. Y. Yoon, J. Hwang, *J. Aerosol Sci.* **2008**, *39*, 460.
[11] a) Y. Zhang, X. Sun, N. Jia, *Sens. Actuator B. Chem.* **2011**, *157*, 527; b) T. Szabó, M. Szekeres, I. Dékány, C. Jackers, S. de Feyter, C. T. Johnston, R. A. Schoonheydt, *J. Phys. Chem. C* **2007**, *111*, 12730; c) Z. Wang, L. Yu, M. Ding, H. Tan, J. Li, Q. Fu, *Polym. Chem.* **2011**, *2*, 601.
[12] L. Wang, Z. Zhang, H. Chen, S. Zhang, C. Xiong, *J. Polym. Res.* **2010**, *17*, 77.
[13] P. Liu, H. Yu, Y. Sun, M. Zhu, Y. Duan, *Biomaterials* **2012**, *33*, 4403.
[14] T. Mecca, G. M. L. Consoli, C. Geraci, R. L. Spina, F. Cunsolo, *Org. Biomol. Chem.* **2006**, *4*, 3763.
[15] a) M. Zhang, M. Liu, Y.-N. Xue, S.-W. Huang, R.-X. Zhuo, *Bioconjugate Chem.* **2009**, *20*, 440; b) C.-H. Wang, C.-W. Chang, C.-A. Peng, *J. Nanopart. Res.* **2011**, *13*, 2749.
[16] K. Ma, M.-X. Hu, Y. Qi, J.-H. Zou, L.-Y. Qiu, Y. Jin, X.-Y. Ying, H.-Y. Sun, *Biomaterials* **2009**, *30*, 6109.
[17] a) J.-H. Kim, J. S. Park, H. N. Yang, D. G. Woo, S. Y. Jeon, H.-J. Do, H.-Y. Lim, J. M. Kim, K.-H. Park, *Biomaterials* **2011**, *32*, 268; b) S. Prabha, W.-Z. Zhou, J. Panyam, V. Labhasetwar, *Int. J. Pharm.* **2002**, *244*, 105; c) F. Sarti, G. Perera, F. Hintzen, K. Kotti, V. Karageorgiou, O. Kammona, C. Kiparissides, A. Bernkop–Schnürch, *Biomaterials* **2011**, *32*, 4052.